



Theoretical uncertainties of (d,³He) and (³He,d) reactions owing to the uncertainties of optical model potentials

Wei-Jia Kong¹ · Dan-Yang Pang²

Received: 16 February 2023 / Revised: 19 April 2023 / Accepted: 21 April 2023 / Published online: 26 June 2023

© The Author(s), under exclusive licence to China Science Publishing & Media Ltd. (Science Press), Shanghai Institute of Applied Physics, the Chinese Academy of Sciences, Chinese Nuclear Society 2023

Abstract

The theoretical uncertainties of single proton transfer cross sections of the (³He,d) and (d,³He) reactions, owing to the uncertainties of the entrance- and exit-channel optical model potentials, are examined with the ³⁰Si(³He,d)³¹P, ¹³B(d,³He)¹²Be, and ³⁴S(³He,d)³⁵Cl reactions at incident energies of 25, 46, and 25 MeV, respectively, within the framework of the distorted wave Born approximation. The differential cross sections at the first peaks in the angular distributions of these reactions are found to have uncertainties of approximately 5%, owing to the uncertainties in the optical model potentials from 20,000 calculations of randomly sampled parameters. This amount of uncertainty is found to be nearly independent of the angular momentum transfer and the target masses within the studied range of incident energies. Uncertainties in the single proton spectroscopic factors obtained by matching the theoretical and experimental cross sections at different scattering angles are also discussed.

Keywords Proton transfer reactions · Optical model potentials · Spectroscopic factors

1 Introduction

Proton transfer reactions, such as (d,³He) and (³He,d) reactions, are important in nuclear physics. They provide not only valuable nuclear reaction data for various applications but also important tools for studying the single-particle structure of atomic nuclei, such as the spectroscopic and asymptotic normalization factors, which are of fundamental importance to nuclear physics and nuclear astrophysics [1–8]. Reaction theories are necessary for extracting such structural information from nuclear reaction measurements [9, 10]. Reliable nuclear structure information relies not only on the precision of measurements but also on the reaction theories used. Experimentalists have always endeavored to make measurements more precise; at the same time, it is

also important to quantify the uncertainties of the theoretical results of the reaction cross sections [11, 12].

In most cases, A(d,³He)B and A(³He,d)B reactions can be well described with the distorted wave Born approximation (DWBA), in which the amplitude is expressed as

$$T_{\beta\alpha}^{DW} = \sum_{nlj} a_{nlj} \int d\mathbf{r}_\alpha \int d\mathbf{r}_\beta \chi_\beta^{(-)*}(\mathbf{k}_\beta, \mathbf{r}_\beta) \phi_{nlj}(\mathbf{R}) V_{tr} f(\mathbf{r}) \chi_\alpha^{(+)}(\mathbf{k}_\alpha, \mathbf{r}_\alpha), \quad (1)$$

where $\chi_\alpha(\mathbf{k}_\alpha, \mathbf{r}_\alpha)$ and $\chi_\beta(\mathbf{k}_\beta, \mathbf{r}_\beta)$ are distorted waves describing the relative motions between the two particles in the entrance and exit channels, which are separated by vectors \mathbf{r}_α and \mathbf{r}_β with wave numbers \mathbf{k}_α and \mathbf{k}_β , respectively. $\phi_{nlj}(\mathbf{R})$ is the normalized single-particle wave function of the transferred proton in the target nucleus, whose associated principal, orbital, and total angular momenta are n , l , and j ; a_{nlj} is the associated spectroscopic amplitude, which is the square root of the spectroscopic factor S_{nlj} . $f(\mathbf{r}) = \langle \psi_{^3\text{He}}(\xi_d, \mathbf{r}) | \Psi_d(\xi_d) \rangle$ is the overlap between the internal wave functions of ³He and deuteron. The post- and prior-forms of the interaction V_{tr} are $U_{dB} + V_{dp} - U_{^3\text{He}B}$ and $V_{dp} + U_{dB} - U_{dA}$, respectively, for an A(d,³He)B reaction, and $V_{dp} + U_{dA} - U_{dB}$ and $U_{dA} + V_{pA} - U_{^3\text{He}A}$, respectively, for an A(³He,d)B reaction. Here, U_{pq} and V_{pq} are the

This work was financially supported by the National Natural Science Foundation of China (No. U2067205).

✉ Dan-Yang Pang
dypang@buaa.edu.cn

¹ School of Physics, Beihang University, Beijing 100191, China

² School of Physics and Beijing Key Laboratory of Advanced Nuclear Materials and Physics, Beihang University, Beijing 100191, China

interactions between particles p and q , with U_{pq} for optical model potentials (OMPs), which are complex valued, and V_{pq} being single-particle binding potentials, which are real. Within the framework of DWBA, the post- and prior-forms are equivalent. For transfer reactions with only one single-particle wave function involved, the cross section is proportional to the spectroscopic factor, that is,

$$\left(\frac{d\sigma}{d\Omega}\right)^{DW} \propto |T_{\beta\alpha}^{DW}|^2 = S_{nlj} \left(\frac{d\sigma}{d\Omega}\right)_{a_{nlj}=1},$$

where $\left(\frac{d\sigma}{d\Omega}\right)_{a_{nlj}=1}$ is the cross section calculated assuming the spectroscopic amplitude to be unity.

Experimentally, the spectroscopic factors are obtained by normalizing $\left(\frac{d\sigma}{d\Omega}\right)_{a_{nlj}=1}$ to the experimental data:

$$S_{nlj} = \left(\frac{d\sigma}{d\Omega}\right)_{\text{exp}} / \left(\frac{d\sigma}{d\Omega}\right)_{a_{nlj}=1}. \quad (2)$$

It is now clear that the spectroscopic factors obtained in this way inherit uncertainties from the uncertainties in both the experimental data and theoretical calculations.

Uncertainties in the theoretical calculations of the transfer reaction cross sections are rooted mainly in the uncertainties of the following: (i) the OMPs, which are responsible for the entrance- and exit-channel distorted waves [χ_α and χ_β in Eq. (1)], (ii) single-particle potential parameters, which are responsible for the single-particle wave functions [ϕ_{nlj} in Eq. (1)], and (iii) the reaction model used, for instance, whether the $f(r)$ term in the transition amplitude is treated exactly or treated with zero-range approximation, and whether the nucleon is assumed to be transferred from one nucleus to another through a direct one-step process only or through higher-order processes such as channel-couplings with nuclear excitations. For a given choice of reaction model, the uncertainties of the theoretical calculations are mainly from uncertainties in the OMPs and single-particle potential parameters.

The parameters of single-particle potentials are usually determined with the separation energy prescription, with which the potential depths are determined by the separation energies of the transferred nucleon when the shape parameters, e.g., the radius parameter r_0 and diffuseness parameter a of a Woods–Saxon (WS) potential, are preselected. For WS potentials, the empirical values $r_0 = 1.25$ fm and $a = 0.65$ fm are frequently used [13], although attempts have been made to determine r_0 with, for instance, (e,e'p) measurements [14] and Hartree–Fock calculations [15–18], with a fixed choice of a .

Optical model potentials are usually phenomenologically determined by requiring them to describe elastic scattering angular distributions [19]. It is well known that potential parameters determined in this way suffer rather

serious uncertainties, especially when only a limited number of experimental data are used to confine these parameters [20, 21]. This situation is better for systematic or global optical model potentials, whose parameters are constrained by experimental data, which cover large ranges of incident energies and target masses. It has been shown that the usage of systematic OMPs helps to reduce the uncertainties of the spectroscopic factors obtained from transfer reactions [5, 22, 23]. Owing to their importance in the study of nuclear reactions and related subjects, such as nuclear structure, nuclear astrophysics, and nuclear applications, much effort has been devoted to the study of systematic optical model potentials [24–26]. However, most references to existing systematic OMPs do not report the uncertainties of their parameters. Fortunately, for the OMPs needed in the study of ($^3\text{He},d$) and ($d,^3\text{He}$) reactions, the recently proposed systematic potentials of ^3He and deuteron are given with uncertainties [27–29]. These uncertainties were obtained using the bootstrap statistical method. The bootstrap method simulates many repeated measurements of the elastic scattering data by creating new datasets of the same size as the original using random sampling with replacement. This procedure was repeated many times, generating the distributions of the OMP parameters, from which the uncertainties of these parameters were obtained. The details of this method can be found in Refs. [24, 27]. These systematic OMPs allow us to quantify the uncertainties of the ($^3\text{He},d$) and ($d,^3\text{He}$) reaction cross sections due to the uncertainties of the optical model potentials.

The reactions analyzed in this study are $^{30}\text{Si}(^3\text{He},d)^{31}\text{P}$ [30, 31], $^{13}\text{B}(d,^3\text{He})^{12}\text{Be}$ [7], and $^{34}\text{S}(^3\text{He},d)^{35}\text{Cl}$ [30, 31]. The angular momentum transfers, which are the same as the orbital angular momentum l of the corresponding single proton wave functions with these three reactions, are $l = 0\hbar$, $1\hbar$, and $2\hbar$, respectively. The incident energies of these reactions were 25, 46, and 25 MeV, respectively. These reactions are analyzed using exact finite-range DWBA, considering the full complex remnant term. The single proton wave function in the ground state of ^3He is calculated with the $p + d$ single-particle potential provided in Ref. [32], which reproduces the $\langle ^3\text{He}|d \rangle$ overlap function calculated with the Green's function Monte-Carlo method [32]. The single proton wave functions in the ground states of target nuclei in the exit channels are determined using the usual separation energy prescription with WS potentials whose radii and diffuseness parameters are $r_0 = 1.25$ fm and $a_0 = 0.65$ fm, respectively. The calculations were performed using the computer code FRESKO [33].

This paper is organized as follows: the forms of OMPs and their parameters are introduced in Sect. 2, the results of our theoretical calculations and the discussion of uncertainties of the differential cross sections at different scattering angles are

discussed in Sect. 3, and the conclusions of this paper are summarized in Sect. 4.

2 Optical model potential parameters

The phenomenological OMPs used in this work are defined as

$$U(r) = -V_r f_{ws}(r) - iW_v f_{ws}(r) - iW_s(-4a_w) \frac{d}{dr} f_{ws}(r) + V_C, \tag{3}$$

where V_r , W_v , and W_s are the depths of the real, volume-imaginary, and surface-imaginary parts of the central potential, respectively. V_C is the Coulomb potential:

$$V_C(r) = \begin{cases} \frac{Z_p Z_T e^2}{r}, & (r > R_C) \\ \frac{Z_p Z_T e^2}{2R_C} \left(3 - \frac{r^2}{R_C^2}\right), & (r \leq R_C), \end{cases} \tag{4}$$

where Z_p and Z_T are the charge numbers of the projectile and target nuclei, respectively, and R_C is the Coulomb radius of the target nuclei. f_{ws} is the WS form factor:

$$f_{ws}(r) = \frac{1}{1 + \exp(r - R_i)/a_i}, \tag{5}$$

where R_i and a_i are the radius and diffuseness parameters, respectively, with $i = r, v$, and s labeling the real, volume-imaginary, and surface-imaginary terms in Eq. 3, respectively. For the OMPs of ³He and deuteron needed by the analysis of (d,³He) and (³He,d) reactions, R_i is calculated with $r_i A_T^{1/3}$, where r_i is the reduced radius parameter and A_T is the mass number of the target nucleus. The OMPs of ³He and deuteron projectiles both have a total set of seven OMP parameters $\{V_r, r_v, a_v, W_v, W_s, r_w, a_w\}$. The uncertainties in these parameters can be obtained from Refs. [27, 29].

3 Uncertainties of the transfer reaction cross sections

The uncertainties in the OMP parameters for ³He and deuteron for the three reactions studied in this work are listed as Δ_p in Table 1. Shown together are the uncertainties in the differential cross sections caused by varying each parameter within their ranges of validity while keeping all other parameters fixed, Δ_σ , and the uncertainties in the differential cross sections caused by varying all of the parameters simultaneously, $\Delta_\sigma(\text{total})$. Note that these OMP parameter uncertainties are given in percentages. For a parameter P ,

Table 1 Uncertainties of the optical model potentials Δ_p , their associated differential cross section uncertainties Δ_σ , and the total uncertainties of the cross sections when all parameters are allowed to vary randomly $\Delta_\sigma(\text{total})$, for the three reactions analyzed in this study

³⁰ Si(³ He,d) ³¹ P reaction ($l = 0$)							
$U_{^3\text{He}}$	V_v	r_v	a_v	W_v	W_s	r_w	a_w
Δ_p (%)	1.12	1.66	1.22	46.7	3.96	3.16	1.19
Δ_σ (%)	0.707	0.224	0.852	0.428	1.52	6.70	2.19
U_d	V_v	r_v	a_v	W_v	W_s	r_w	a_w
Δ_p (%)	0.964	0.151	0.129	12.2	28.6	0.390	0.134
Δ_σ (%)	0.669	0.036	0.064	0.377	2.39	0.405	0.057
$\Delta_\sigma(\text{total})$ (%)	4.48						
¹³ B(d, ³ He) ¹² Be reaction ($l = 1$)							
$U_{^3\text{He}}$	V_v	r_v	a_v	W_v	W_s	r_w	a_w
Δ_p (%)	1.14	2.20	1.22	42.3	6.51	3.99	1.19
Δ_σ (%)	0.416	1.49	0.440	1.25	4.11	7.37	2.32
U_d	V_v	r_v	a_v	W_v	W_s	r_w	a_w
Δ_p (%)	1.38	0.192	0.129	6.18	123	0.321	0.134
Δ_σ (%)	0.712	0.230	0.147	1.41	0.114	0.383	0.059
$\Delta_\sigma(\text{total})$ (%)	5.27						
³⁴ S(³ He,d) ³⁵ Cl reaction ($l = 2$)							
$U_{^3\text{He}}$	V_v	r_v	a_v	W_v	W_s	r_w	a_w
Δ_p (%)	1.11	1.56	1.22	47.7	3.97	3.15	1.19
Δ_σ (%)	0.144	0.678	0.169	1.17	2.27	7.47	2.26
U_d	V_v	r_v	a_v	W_v	W_s	r_w	a_w
Δ_p (%)	0.960	0.151	0.129	13.7	27.1	0.400	0.134
Δ_σ (%)	0.037	0.124	0.121	1.61	3.24	0.470	0.067
$\Delta_\sigma(\text{total})$ (%)	5.21						

See the text for details

whose mean value is \bar{P} and absolute uncertainty is ΔP , its uncertainty, in percentage, is

$$\Delta_p = \frac{\Delta P}{\bar{P}} \times 100\%.$$

The absolute uncertainties of these parameters can be found in Ref. [27] for ${}^3\text{He}$ and Ref. [29] for deuteron. The uncertainties of the calculated differential cross sections are defined in the same way. The uncertainties are evaluated at the center-of-mass angles $\theta_{\text{c.m.}} = 0^\circ, 9^\circ, \text{ and } 13^\circ$ for the ${}^{30}\text{Si}({}^3\text{He},\text{d}){}^{31}\text{P}$, ${}^{13}\text{B}(\text{d},{}^3\text{He}){}^{12}\text{Be}$, and ${}^{34}\text{S}({}^3\text{He},\text{d}){}^{35}\text{Cl}$ reactions, respectively, where their maximum differential cross sections occur. Within the ranges of these parameters, the cross sections depend nearly linearly on the values of each individual parameter. Thus, when one parameter, p , is changed within the range $[(1 - \Delta_p) \times p, (1 + \Delta_p) \times p]$ while keeping all other parameters fixed, the differential cross section will vary between its upper and lower limits, σ_{max} and σ_{min} , respectively. Δ_σ (in %) is defined as $100\% \times (\sigma_{\text{max}} - \sigma_{\text{min}}) / (\sigma_{\text{max}} + \sigma_{\text{min}})$.

In contrast to how the differential cross sections depend almost linearly on each of the parameters within their uncertainties (when all other parameters are fixed), they tend to follow a Gaussian distribution when all the OMP parameters are varied simultaneously. As an example, Fig. 1 shows the distributions of the differential cross sections for the three reactions at their first three peak angles. The cross sections are normalized to their mean values: $\delta_\sigma = (\sigma - \bar{\sigma}) / \bar{\sigma}$, where $\bar{\sigma}$ are the mean values. Figure 1 shows the results of 20,000 calculations, each with the parameter sets $\{V_r, r_v, a_v, W_v, W_s, r_w, a_w\}$ randomly sampled within their individual uncertainties. Uniform random numbers were used for this procedure. This number of samples is sufficient for our analysis because

the results are nearly the same as those with 10000 samples. Uncertainties of differential cross sections when all the OMP parameters vary simultaneously, $\Delta_{\sigma,\text{total}}$, are taken to be the standard deviations of these distributions, approximated by the standard deviations of the Gaussian function that best fits these distributions in Fig. 1. The $\Delta_{\sigma,\text{total}}$ values for the ${}^{30}\text{Si}({}^3\text{He},\text{d}){}^{31}\text{P}$, ${}^{13}\text{B}(\text{d},{}^3\text{He}){}^{12}\text{Be}$, and ${}^{34}\text{S}({}^3\text{He},\text{d}){}^{35}\text{Cl}$ reactions at scattering angles of $0^\circ, 9^\circ, \text{ and } 13^\circ$, respectively, are listed in Table 1.

From Table 1, the following observations are made: (1) the uncertainties of OMPs in both exit- and entrance-channels result in an uncertainty of around 5% in the $({}^3\text{He},\text{d})$ and $(\text{d},{}^3\text{He})$ reactions, which seems to be independent of the angular momentum transfer, the target masses, and the incident energies; (2) $\Delta_{\sigma,\text{total}}$ are smaller than the sums of Δ_σ for all the three reactions, suggesting that some correlations exist among the effects of uncertainties induced by different parameters; and (3) among all these parameters, the radius and diffuseness parameters of the imaginary potentials r_w and a_w of the ${}^3\text{He}$ potential are the most sensitive to the transfer reactions. The uncertainties in the cross sections caused by these two parameters are approximately twice the uncertainties in the parameters themselves. This suggests that these two parameters should be the focus of future systematic OMP studies to further reduce the theoretical uncertainties of the $({}^3\text{He},\text{d})$ and $(\text{d},{}^3\text{He})$ reactions.

Experimentally, spectroscopic factors studied with transfer reactions are usually obtained by matching the theoretical cross sections to the experimental ones at the peaks of the angular distributions. This is a reasonable choice because at these angles, the differential cross sections are at their maximum values, which means that their experimental uncertainties, at least the statistical uncertainties, are the smallest. The spectroscopic factors obtained at these angles have minimum

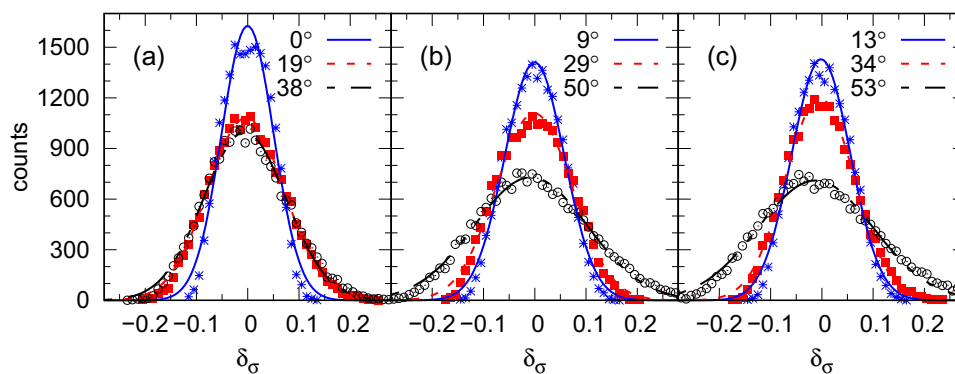


Fig. 1 (Color online) Distributions of the normalized cross sections as results of calculations, randomly sampled 20,000 times, of the OMP parameters at the three peaks of the angular distributions for the **a** ${}^{30}\text{Si}({}^3\text{He},\text{d}){}^{31}\text{P}$, **b** ${}^{13}\text{B}(\text{d},{}^3\text{He}){}^{12}\text{Be}$, and **c** ${}^{34}\text{S}({}^3\text{He},\text{d}){}^{35}\text{Cl}$ reactions at incident energies of 25, 46, and 25 MeV, respectively. The scattering angles indicated in these figures are in center-of-mass sys-

tems. The curves represent the Gaussian functions whose heights and width parameters are found to best fit these distributions. The Y-axis is the number of cases whose normalized cross sections δ_σ fall in the intervals of $[\delta_\sigma - \Delta_{\delta_\sigma}/2, \delta_\sigma + \Delta_{\delta_\sigma}/2]$ with $\Delta_{\delta_\sigma} = 0.01$. See the text for details

experimental uncertainties. However, cross sections at the first peaks may not always be available experimentally. In those cases, the spectroscopic factors must be obtained using experimental data at the second or even the third peaks. It is interesting to determine the extent to which the uncertainties of the spectroscopic factors will increase in such cases. This information is shown in Fig. 1 where the distributions of cross sections at the second and the third peaks are given for the three reactions analyzed in this study, which have angular momentum transfers l of $0\hbar$, $1\hbar$, and $2\hbar$, respectively. For the $^{30}\text{Si}(^3\text{He,d})^{31}\text{P}$ reaction, which has $l = 0\hbar$, the uncertainties of cross sections at the second and third peaks are nearly the same, which are 7.5% on average, larger than that with the first peak by a factor of 68%. However, for the $^{13}\text{B}(d,^3\text{He})^{12}\text{Be}$ and $^{34}\text{S}(^3\text{He,d})^{35}\text{Cl}$ reactions that have $l = 1\hbar$ and $2\hbar$, respectively, the uncertainties of the cross sections at their first and second peaks are rather close, 6.0% and 5.8%, respectively, much smaller than those of their third peaks, which are around 11.0%. Whether these results apply generally for all reactions at all incident energies might be an interesting subject for further study.

The uncertainties of the theoretical cross sections at different scattering angles are more clearly seen in Fig. 2, in which the uncertainties caused by the uncertainties in the OMP parameters are depicted as shaded bands for the three reactions analyzed in this study. The widths of these bands represent the upper and lower bounds of the cross sections at each scattering angle. The corresponding uncertainties in percentage are shown by the brown curves with values shown by the vertical ordinate on the right. The following conclusions can be drawn from this figure: (1) within their ranges of uncertainties, as shown in Table 1, variations of the OMP parameters mainly affect the amplitudes of the differential cross sections and do not change the angular distributions, especially at smaller angles where theoretical cross sections are compared with experimental ones to get the spectroscopic factors; and (2) the uncertainties of differential cross sections increase with increasing scattering angles. Further, the theoretical uncertainties at the shoulders of the peaks may be even smaller than those at the peak angles. However, these shoulders are where the differential cross sections change most abruptly with respect to the scattering angles. Spectroscopic factors obtained by matching the theoretical and experimental cross sections at these angles will have the disadvantage that they will need to have much higher angular resolutions than those measured at the peaks.

4 Summary

In summary, (³He,d) and (d,³He) reactions are important tools for studying the single-particle structure of atomic nuclei. Knowledge of the uncertainties in the theoretical

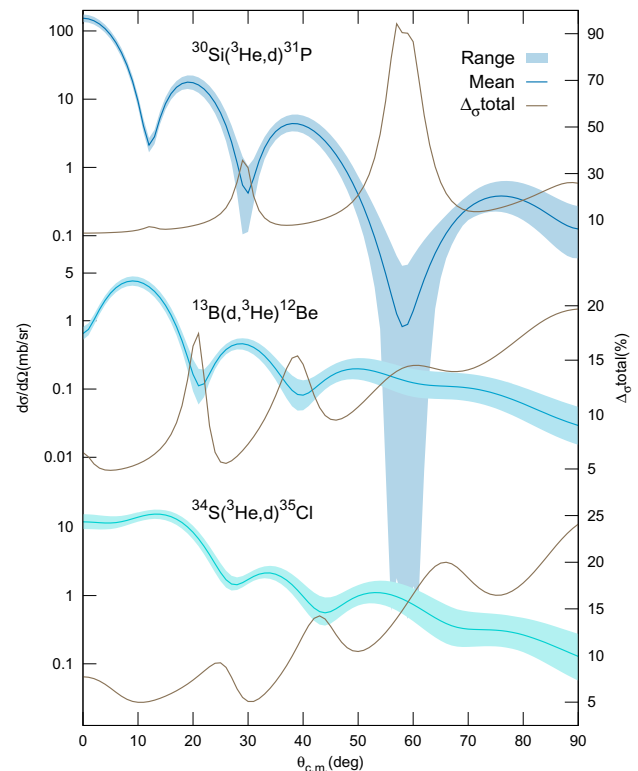


Fig. 2 (Color online) Uncertainty of the $^{30}\text{Si}(^3\text{He,d})^{31}\text{P}$, $^{13}\text{B}(d,^3\text{He})^{12}\text{Be}$, and $^{34}\text{S}(^3\text{He,d})^{35}\text{Cl}$ reactions due to the uncertainties in the OMP parameters of both the entrance and exit channels. The widths of the bands represent the upper and lower bounds of the cross sections (in mb/sr), which are the results of randomly sampling the OMP parameters 20,000 times. The brown curves are their corresponding uncertainties in percentage, whose values are given by the right y-axis

calculations for these reactions is important for nuclear structure information, such as spectroscopic factors, obtained from these reactions. This study analyzed the uncertainties of theoretical cross sections, owing to the uncertainties in the entrance- and exit-channel optical model potentials, for these reactions. The systematic potential of ³He and deuteron projectiles were used, whose parameter uncertainties were available in Refs. [27] and [29], respectively. Three reactions, $^{30}\text{Si}(^3\text{He,d})^{31}\text{P}$, $^{13}\text{B}(d,^3\text{He})^{12}\text{Be}$, and $^{34}\text{S}(^3\text{He,d})^{35}\text{Cl}$, at incident energies of 25, 46, and 25 MeV, respectively, were analyzed within the framework of an exact finite-range DWBA. The momentum transfers of these chosen reactions were $0\hbar$, $1\hbar$, and $2\hbar$, respectively. The analysis was performed through 20,000 calculations, for each reaction, randomly sampling the entrance- and exit-channel parameters simultaneously. It was found that the uncertainties of the theoretical cross sections of these reactions caused by the uncertainties in the OMP parameters were around 5% at scattering angles where the reactions have the largest cross sections. Uncertainties in the single proton spectroscopic factors with these reactions were concluded to be the same,

owing to the uncertainties in the OMP parameters. Such uncertainties seem to be independent of the angular momentum transfer and the target masses for the range of incident energies analyzed in this study.

Author Contributions All authors contributed to work in this paper. Data collection and analysis were performed by Wei-Jia Kong and Dan-Yang Pang. The first draft of the manuscript was written by Dan-Yang Pang and all authors commented on previous versions of the manuscript. All authors read and approved the final manuscript.

Data availability The data that support the findings of this study are openly available in Science Data Bank at <https://www.doi.org/10.57760/sciencedb.j00186.00011> and <https://cstr.cn/31253.11.sciencedb.j00186.00011>.

Declarations

Conflict of interest The authors declare that they have no competing interests.

References

- P. Bém, V. Burjan, V. Kroha et al., Asymptotic normalization coefficients for $^{14}\text{N} \leftrightarrow ^{13}\text{C} + p$ from $^{13}\text{C}(^3\text{He}, d)^{14}\text{N}$. *Phys. Rev. C* **62**, 024320 (2000). <https://doi.org/10.1103/PhysRevC.62.024320>
- A.M. Mukhamedzhanov, P. Bém, V. Burjan et al., Asymptotic normalization coefficients from the $^{20}\text{Ne}(^3\text{He}, d)^{21}\text{Ne}$ reaction and astrophysical factor for $^{20}\text{Ne}(p, \gamma)^{21}\text{Na}$. *Nucl. Phys. Rev. C* **73**, 035806 (2006). <https://doi.org/10.1103/PhysRevC.73.035806>
- N. Burtebayev, J.T. Burtebayeva, N.V. Glushchenko et al., Effects of t - and α -transfer on the spectroscopic information from the $^6\text{Li}(^3\text{He}, d)^7\text{Be}$ reaction. *Nucl. Phys. A* **909**, 20 (2013). <https://doi.org/10.1016/j.nuclphysa.2013.04.008>
- C. Wen, Y.P. Xu, D.Y. Pang et al., Quenching of neutron spectroscopic factors of radioactive carbon isotopes with knockout reactions within a wide energy range. *Chin. Phys. C* **41**, 054104 (2017). <https://doi.org/10.1088/1674-1137/41/5/054104>
- W. Liu, J.L. Lou, Y.L. Ye et al., Experimental study of intruder components in light neutron-rich nuclei via single-nucleon transfer reaction. *Nucl. Sci. Tech.* **31**, 20 (2020). <https://doi.org/10.1007/s41365-020-0731-y>
- T. Aumann, C. Barbieri, D. Bazin et al., Quenching of single-particle strength from direct reactions with stable and rare-isotope beams. *Prog. Part. Nucl. Phys.* **118**, 103847 (2021). <https://doi.org/10.1016/j.pnpnp.2021.103847>
- W. Liu, J.L. Lou, Y.L. Ye et al., New investigation of low-lying states in ^{12}Be via $a^2\text{H}(^{13}\text{B}, ^3\text{He})$ reaction. *Phys. Rev. C* **105**, 034613 (2022). <https://doi.org/10.1103/PhysRevC.105.034613>
- B.P. Kay, T.L. Tang, I.A. Tolstukhin et al., Quenching of single-particle strength in $A = 15$ nuclei. *Phys. Rev. Lett.* **129**, 152501 (2022). <https://doi.org/10.1103/PhysRevLett.129.152501>
- R.J. Philpott, W.T. Pinkston, G.R. Satchler, Some studies of realistic form factors for nucleon-transfer reactions. *Nucl. Phys. A* **119**, 241 (1968). [https://doi.org/10.1016/0375-9474\(68\)90300-X](https://doi.org/10.1016/0375-9474(68)90300-X)
- R.C. Johnson, Theory of the $A(d, p)B$ reaction as a tool for nuclear structure studies. *J. Phys. G Nucl. Part. Phys.* **41**, 094005 (2014). <https://doi.org/10.1088/0954-3899/41/9/094005>
- J.D. McDonnell, N. Schunck, D. Higinbotham et al., Uncertainty quantification for nuclear density functional theory and information content of new measurements. *Phys. Rev. Lett.* **114**, 122501 (2015). <https://doi.org/10.1103/PhysRevLett.114.122501>
- A.E. Lovell, F.M. Nunes, M. Catacora-Rios et al., Recent advances in the quantification of uncertainties in reaction theory. *J. Phys. G Nucl. Part. Phys.* **48**, 014001 (2021). <https://doi.org/10.1088/1361-6471/abba72>
- M.B. Tsang, J. Lee, S.C. Su et al., Survey of excited state neutron spectroscopic factors for $Z = 8 - 28$ nuclei. *Phys. Rev. Lett.* **102**, 062501 (2009). <https://doi.org/10.1103/PhysRevLett.102.062501>
- C.J. Kramer, H.P. Blok, L. Lapikas, A consistent analysis of $(e, e'p)$ and $(d, ^3\text{He})$ experiments. *Nucl. Phys. A* **679**, 267 (2001). [https://doi.org/10.1016/S0375-9474\(00\)00379-1](https://doi.org/10.1016/S0375-9474(00)00379-1)
- A. Gade, P. Adrich, D. Bazin et al., Reduction of spectroscopic strength: weakly-bound and strongly-bound single-particle states studied using one-nucleon knockout reactions. *Phys. Rev. C* **77**, 044306 (2008). <https://doi.org/10.1103/PhysRevC.77.044306>
- J.A. Tostevin, A. Gade, Systematics of intermediate-energy single-nucleon removal cross-sections. *Phys. Rev. C* **90**, 057602 (2014). <https://doi.org/10.1103/PhysRevC.90.057602>
- J.A. Tostevin, A. Gade, Updated systematics of intermediate-energy single-nucleon removal cross-sections. *Phys. Rev. C* **103**, 054610 (2021). <https://doi.org/10.1103/PhysRevC.103.054610>
- Y.P. Xu, D.Y. Pang, X.Y. Yun et al., Proton-neutron asymmetry independence of reduced single-particle strengths derived from (p, d) reactions. *Phys. Lett. B* **790**, 308 (2019). <https://doi.org/10.1016/j.physletb.2019.01.034>
- W. Nan, B. Guo, C.J. Lin et al., First proof-of-principle experiment with the post-accelerated isotope separator on-line beam at BRIF: measurement of the angular distribution of $^{23}\text{Na} + ^{40}\text{Ca}$ elastic scattering. *Nucl. Sci. Tech.* **32**, 53 (2021). <https://doi.org/10.1007/s41365-021-00889-9>
- H. Leeb, E.W. Schmid, A physical interpretation of the discrete ambiguities in the optical potential for composite particles. *Z. Physik A* **296**, 51 (1980). <https://doi.org/10.1007/BF01415614>
- M.E. Brandan, S.H. Fricke, K.W. McVoy, Resolution of potential ambiguities through farside angular structure: data summary. *Phys. Rev. C* **38**, 673 (1988). <https://doi.org/10.1103/PhysRevC.38.673>
- X.D. Liu, M.A. Famiano, W.G. Lynch et al., Systematic extraction of spectroscopic factors from $^{12}\text{C}(d, p)^{13}\text{C}$ and $^{13}\text{C}(p, d)^{12}\text{C}$ reactions. *Phys. Rev. C* **69**, 064313 (2004). <https://doi.org/10.1103/PhysRevC.69.064313>
- X.Y. Yun, D.Y. Pang, Y.P. Xu et al., What kind of optical model potentials should be used for deuteron stripping reactions? *Sci. China Phys. Mech. Astron.* **63**, 222011 (2020). <https://doi.org/10.1007/s11433-019-9389-6>
- R.L. Varner, W.J. Thompson, T.L. McAbee et al., A global nucleon optical model potential. *Phys. Rep.* **201**, 57 (1991). [https://doi.org/10.1016/0370-1573\(91\)90039-0](https://doi.org/10.1016/0370-1573(91)90039-0)
- A.J. Koning, J.P. Delaroche, Local and global nucleon optical models from 1 keV to 200 MeV. *Nucl. Phys. A* **713**, 231 (2003). [https://doi.org/10.1016/S0375-9474\(02\)01321-0](https://doi.org/10.1016/S0375-9474(02)01321-0)
- Y.L. Xu, H.R. Guo, Y.L. Han et al., Helium-3 global optical model potential with energies below 250 MeV. *Sci. China Phys. Mech. Astron.* **54**, 2005 (2011). <https://doi.org/10.1007/s11433-011-4488-5>
- D.Y. Pang, P. Roussel-Chomaz, H. Savajols et al., Global optical model potential for $A = 3$ projectiles. *Phys. Rev. C* **79**, 024615 (2009). <https://doi.org/10.1103/PhysRevC.79.024615>
- D.Y. Pang, W.M. Dean, A.M. Mukhamedzhanov, Optical model potential of $A = 3$ projectiles for $1p$ -shell nuclei. *Phys. Rev. C* **91**, 024611 (2015). <https://doi.org/10.1103/PhysRevC.91.024611>
- Y. Zhang, D.Y. Pang, J.L. Lou, Optical model potential for deuteron elastic scattering with $1p$ -shell nuclei. *Phys. Rev. C* **94**, 014619 (2016). <https://doi.org/10.1103/PhysRevC.94.014619>
- J. Veronite, G. Berrier-Ronsin, J. Kalifa et al., Spectroscopic factors from one-proton stripping reactions on sd -shell nuclei:

- experimental measurements and shell-model calculations. Nucl. Phys. A **571**, 1 (1994). [https://doi.org/10.1016/0375-9474\(94\)90339-5](https://doi.org/10.1016/0375-9474(94)90339-5)
31. J. Lee, D.Y. Pang, Y.L. Han et al., Proton spectroscopic factors deduced from Helium-3 global phenomenological and microscopic optical model potentials. Chin. Phys. Lett. **31**, 092103 (2014). <https://doi.org/10.1088/0256-307X/31/9/092103>
32. I. Brida, Steven C. Pieper, R.B. Wiringa, Quantum Monte Carlo calculations of spectroscopic overlaps in $A \leq 7$ nuclei. Phys. Rev. C **84**, 024319 (2011). <https://doi.org/10.1103/PhysRevC.84.024319>
33. I.J. Thompson, Coupled reaction channels calculations in nuclear physics. Comput. Phys. Rep. **7**, 167 (1988). [https://doi.org/10.1016/0167-7977\(88\)90005-6](https://doi.org/10.1016/0167-7977(88)90005-6)

Springer Nature or its licensor (e.g. a society or other partner) holds exclusive rights to this article under a publishing agreement with the author(s) or other rightsholder(s); author self-archiving of the accepted manuscript version of this article is solely governed by the terms of such publishing agreement and applicable law.